Neuron
Article

Bassoon Specifically Controls Presynaptic P/Q-type Ca^{2+} Channels via RIM-Binding Protein

Daria Davydova,[1,7,9] Claudia Marini,[1,7] Claire King,[4] Julia Klueva,[2] Ferdinand Bischof,[1] Stefano Romorini,[1] Carolina Montenegro-Venegas,[1] Martin Heine,[2] Romy Schneider,[2] Markus S. Schröder,[1] Wilko D. Altrock,[1,5] Christian Henneberger,[4,6] Dmitri A. Rusakov,[4] Eckart D. Gundelfinger,[1,5,8,*] and Anna Fejtova[1,3,8,*]
[1]Department of Neurochemistry/Molecular Biology
[2]Molecular Physiology Group
[3]Presynaptic Plasticity Group
Leibniz Institute for Neurobiology, 39118 Magdeburg, Germany
[4]Institute of Neurology, University College London, London WC1N 3BG, UK
[5]Center for Behavioral Brain Sciences and Medical Faculty, Otto von Guericke University, 39118 Magdeburg, Germany
[6]Institute of Cellular Neuroscience, Medical Faculty, University of Bonn, 53127 Bonn, Germany
[7]Co-first author
[8]Co-senior author
[9]Present address: Department of Women's and Children's Health, Karolinska University Hospital, 171 77 Stockholm, Sweden
*Correspondence: gundelfi@lin-magdeburg.de (E.D.G.), afejtova@lin-magdeburg.de (A.F.)
http://dx.doi.org/10.1016/j.neuron.2014.02.012

SUMMARY

Voltage-dependent Ca^{2+} channels (Ca_Vs) represent the principal source of Ca^{2+} ions that trigger evoked neurotransmitter release from presynaptic boutons. Ca^{2+} influx is mediated mainly via $Ca_V2.1$ (P/Q-type) and $Ca_V2.2$ (N-type) channels, which differ in their properties. Their relative contribution to synaptic transmission changes during development and tunes neurotransmission during synaptic plasticity. The mechanism of differential recruitment of $Ca_V2.1$ and $Ca_V2.2$ to release sites is largely unknown. Here, we show that the presynaptic scaffolding protein Bassoon localizes specifically $Ca_V2.1$ to active zones via molecular interaction with the RIM-binding proteins (RBPs). A genetic deletion of Bassoon or an acute interference with Bassoon-RBP interaction reduces synaptic abundance of $Ca_V2.1$, weakens P/Q-type Ca^{2+} current-driven synaptic transmission, and results in higher relative contribution of neurotransmission dependent on $Ca_V2.2$. These data establish Bassoon as a major regulator of the molecular composition of the presynaptic neurotransmitter release sites.

INTRODUCTION

Evoked neurotransmitter release from presynaptic boutons is based on depolarization-induced fusion of synaptic vesicles (SV) with the cell membrane at the active zone. The mediator between membrane depolarization and SV exocytosis is the diffusible Ca^{2+} ion, which enters the presynaptic boutons through voltage-dependent Ca^{2+} channels (Ca_Vs) (Catterall and Few, 2008). The density of Ca_Vs at the active zone is a major determinant of the presynaptic efficacy of individual synapses (Sheng et al., 2012). Due to the relatively low intracellular level of free Ca^{2+}, there is a steep concentration gradient around the open Ca_V pores. Rapid and reliable synchronous release of neurotransmitter therefore requires exact localization of Ca_Vs relative to the exocytic machinery, which is achieved by a process named positional priming (Neher and Sakaba, 2008). The components of the presynaptic cytomatrix at the active zone (CAZ), in particular Rab3-interacting molecule (RIM) and RIM-binding protein (RBP), and the $\alpha2\delta$ and β auxiliary subunits of Ca_Vs control the abundance and positional priming of Ca_Vs at the synapse in *Caenorhabditis elegans*, in *Drosophila*, and in mammals (Graf et al., 2012; Gundelfinger and Fejtova, 2012; Hibino et al., 2002; Hoppa et al., 2012; Kaeser et al., 2011; Kiyonaka et al., 2007; Liu et al., 2011; Saheki and Bargmann, 2009; Südhof, 2012). At hippocampal synapses, $Ca_V2.1$ and $Ca_V2.2$ pore-forming subunit-containing channels are the main presynaptic sources of Ca^{2+} influx mediating P/Q- and N-type currents, respectively (Luebke et al., 1993; Takahashi and Momiyama, 1993). The proportional contribution of $Ca_V2.1$ and $Ca_V2.2$ to neurotransmitter release varies among individual synapses (Ariel et al., 2012) and decisively shapes synaptic transmission and plasticity (Ahmed and Siegelbaum, 2009; Fedchyshyn and Wang, 2005). Interference with RIM, $\alpha2\delta$, and β equally affects the localization of both abundant presynaptic Ca_Vs (Han et al., 2011; Hoppa et al., 2012; Kaeser et al., 2011) raising questions about mechanisms of differential recruitment of $Ca_V2.1$ and $Ca_V2.2$ to release sites, which mechanistically underlies rapid changes of presynaptic efficacy during synaptic plasticity (Ahmed and Siegelbaum, 2009).

Here, we report on the physical interaction of the presynaptic CAZ protein Bassoon with RBP. Via this interaction, Bassoon functions in localizing of $Ca_V2.1$, without affecting the positioning of $Ca_V2.2$. Interference with Bassoon expression or its interaction with RBP affects synaptic recruitment of $Ca_V2.1$ and eventually decreases the relative contribution of $Ca_V2.1$-mediated synaptic transmission. We suggest that Bassoon controls the molecular composition of release sites through specific functional capturing of $Ca_V2.1$ and thereby contributes to the determination of presynaptic efficacy of individual synapses.

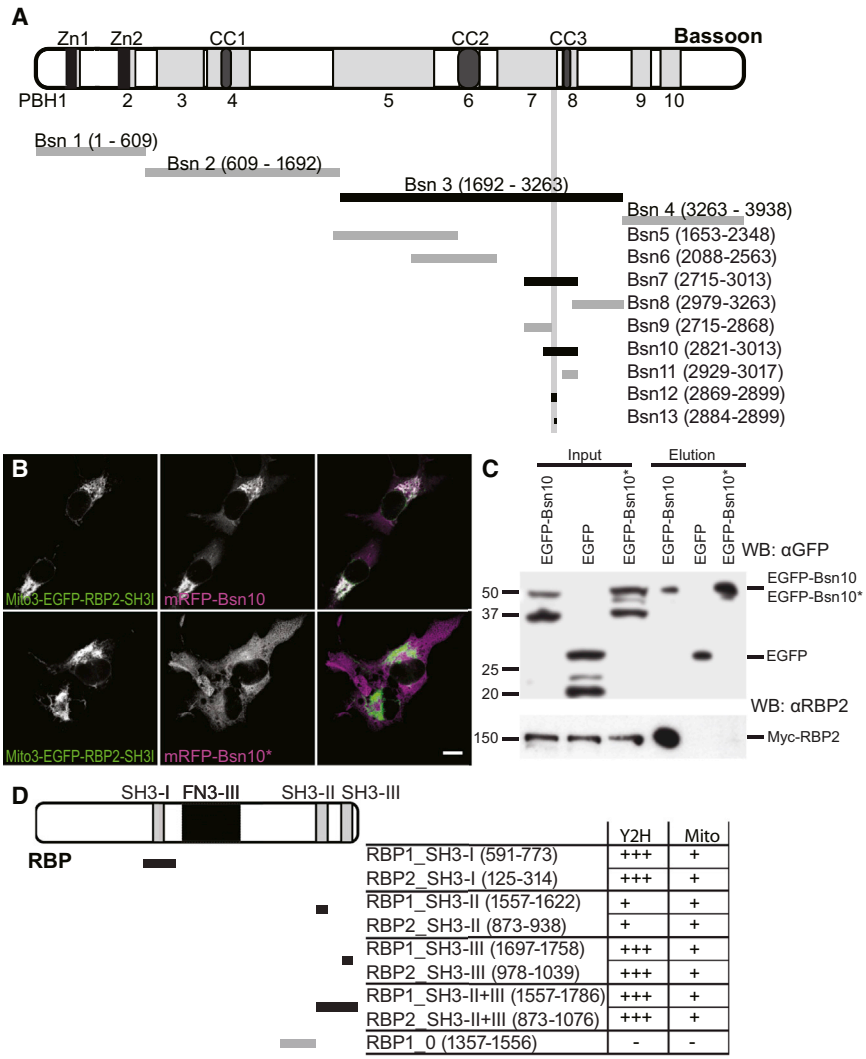

	Y2H	Mito
RBP1_SH3-I (591-773)	+++	+
RBP2_SH3-I (125-314)	+++	+
RBP1_SH3-II (1557-1622)	+	+
RBP2_SH3-II (873-938)	+	+
RBP1_SH3-III (1697-1758)	+++	+
RBP2_SH3-III (978-1039)	+++	+
RBP1_SH3-II+III (1557-1786)	+++	+
RBP2_SH3-II+III (873-1076)	+++	+
RBP1_0 (1357-1556)	-	-

Figure 1. Bassoon Interacts with RBPs

(A) The position of the RBP-interaction interface in Bassoon and the extension of Bassoon fragments used in Y2H screening and interaction studies are depicted. Black bars represent constructs interacting with SH3 domain-containing constructs of RBP1 and RBP2.

(B) Recruitment assay in COS7 cells with mito-targeted EGFP-RBP2-SH3I for mRFP-Bsn10 bearing the RBP-binding motif, but not with mRFP-Bsn10* containing three point mutations in the binding motif (RTLPSPP → ATLASPA; see also Figure S1). Scale bar represents 10 μm.

(C) Myc-RBP2 can be coimmunoprecipitated with GFP antibodies when coexpressed with EGFP-Bsn10, but not with EGFP-Bsn10* or with EGFP alone. Antibodies used for immunodetection on western blots (WB), position of bands corresponding to proteins of interest and size markers are indicated.

(D) Binding characteristics of RBP-SH3 domains to the RTLPSPP motif of Bassoon in Y2H and mito-targeting assays.

Abbreviations: Zn1/2, zinc fingers; CC1-3, coiled-coil regions; PBH1-10, Piccolo-Bassoon homology regions; SH3, src homology domain 3; FNIII, three contiguous fibronectin-type III domains, numbers in brackets correspond to included aa residues of rat Bassoon and RBPs.

RESULTS

SH3 Domains of RBP Interact with PXXP Motif of Bassoon

Initially, we isolated a RBP1 clone bearing sequence downstream of amino acid residues (aa) 1,357 in a yeast-2-hybrid (Y2H) screen with the bait fragment Bsn7 covering aa 2,715–3,013 of rat Bassoon. In subsequent Y2H system-based interaction assays we narrowed down the interacting region to the RTLPSPP sequence (aa 2,889–2,895) of Bassoon, which resembles the consensus interaction motif (RXΦPXΦP) for class-I src homology 3 (SH3) domains (Mayer, 2001) (Figure 1A). Consistently, mutation of the RBP-binding site within Bassoon to ATLASPA abolished the interaction completely both in Y2H and cellular corecruitment assays (Figure 1B and Figure S1 available online). The mutation also interfered with coimmunoprecipitation of fragment Bsn10 (aa 2,821–3,013) with overexpressed RBP2 in HEK293T cells (Figure 1C). RBPs contain an N-terminal SH3I and a tandem of SH3II+SH3III domains at the C terminus (Figure 1D). SH3I and single and tandem SH3II+III domains of RBPs bind to Bassoon in Y2H and in cellular corecruitment assays (Figures 1D and S1).

RBP Can Link Bassoon with Ca_Vs

SH3 domains of RBPs bind to the PXXP motif in the C-terminal region of the α1 pore-forming subunit of retinal presynaptic L-type channels ($Ca_V1.3$). This motif is conserved in $Ca_V2.1$ and $Ca_V2.2$ (Figure 2A) (Hibino et al., 2002). RBPs having multiple SH3 domains are potentially capable to interact simultaneously with Ca_Vs and Bassoon to function as a molecular linker between the presynaptic cytomatrix and Ca^{2+} channels. To test this hypothesis, we performed coimmunoprecipitations from HEK293T cells expressing PXXP motif containing fragments of Bassoon (mRFP-Bsn10) and $Ca_V2.1$ (EGFP-$Ca_V2.1$) and myc-tagged full-length RBP2 using specific GFP antibodies. HEK293T cells do not express Bassoon, $Ca_V2.1$, or RBP2 endogenously. We could efficiently coprecipitate the Bassoon fragment with EGFP-$Ca_V2.1$ only when RBP2 was coexpressed, confirming that RBP2 can interact with PXXP motifs of Bassoon and $Ca_V2.1$ and function as a molecular linker between these proteins (Figure 2B). Further, we expressed EGFP-Bsn10 and its RBP binding-deficient mutant (EGFP-Bsn10*), which differs only by the substitution of 3 aa in the RBP-binding motif (RTLPSPP → ATLASPA), together with myc-tagged full-length RBP2 and PXXP motif-containing fragment of $Ca_V2.1$ in COS7 cells, which also do not express detectable levels of Bassoon, $Ca_V2.1$, or RBP2 endogenously.

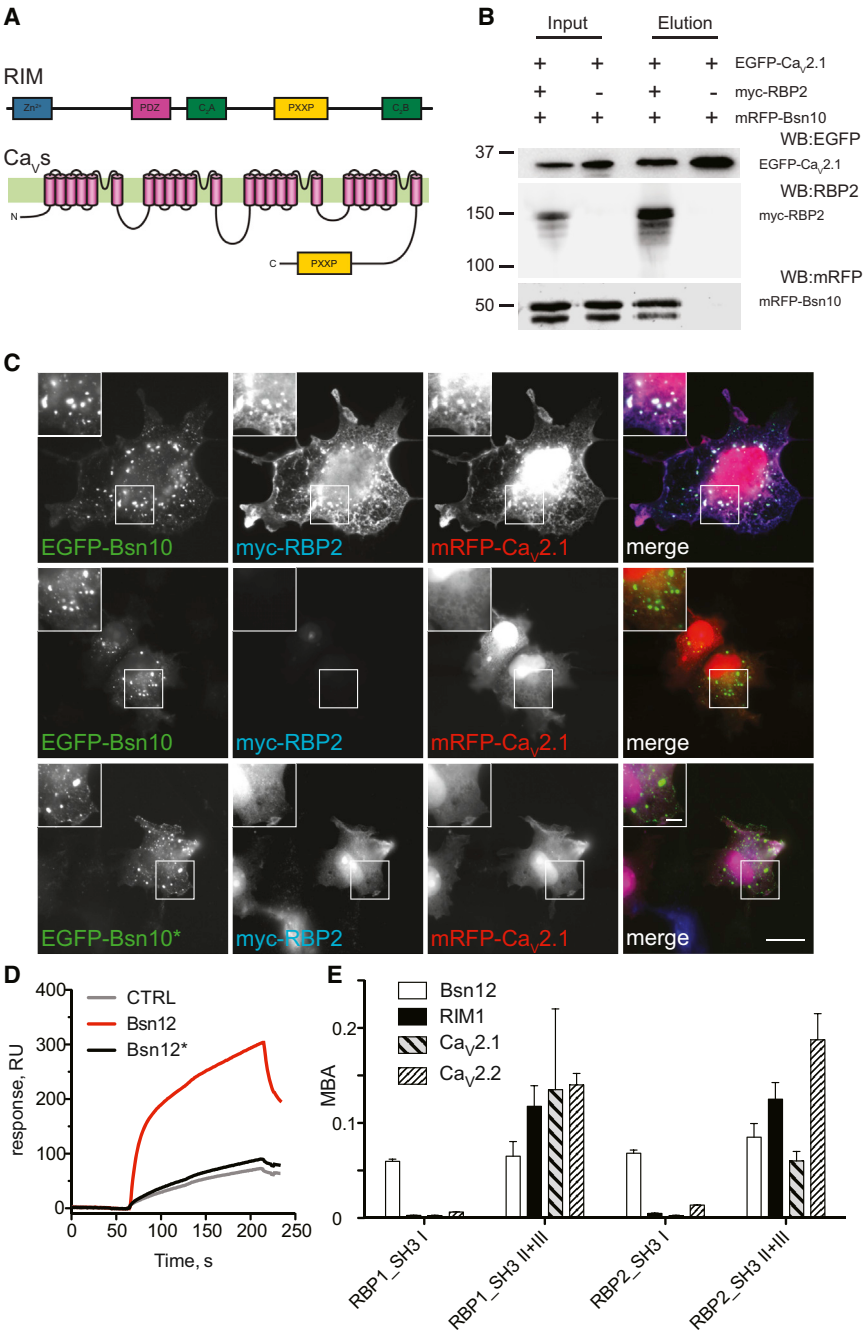

Figure 2. RBP Can Physically Link Bassoon with $Ca_V2.1$

(A) Domain structure of RIMs (α-isoforms with Zn-zinc fingers, PDZ domain, C2 domains C2A and C2B) and of Ca_Vs; locations of RBP-binding PXXP motifs are indicated.

(B) Coexpression of RBP2 is required to coprecipitate PXXP motif-bearing recombinant fragments of Bassoon and $Ca_V2.1$ from HEK293T cell lysates with GFP antibodies. Size markers are given in kDa.

(C) PXXP-motif-containing fragment of $Ca_V2.1$ is recruited by Bsn10 only when full-length RBP2 is coexpressed in COS7 cells (upper row). Absence of RBP2 or mutation of the PXXP motif in Bsn10* interferes with corecruitment of $Ca_V2.1$ (middle and lower row, respectively). Regions in squares are shown magnified in the upper left insert of each image. Scale bar represents 20 μm in overview and 5 μm in inset.

(D) Sensorgrams showing binding and dissociation of RBP2-SH3I from chip with immobilized His-Trx, Bsn10, and mutated Bsn10* proteins.

(E) Quantification of in vitro binding of SH3I or SH3II+III of RBPs to immobilized PXXP-containing motifs of Bsn, RIM1, $Ca_V2.1$, and $Ca_V2.2$. Bars represent mean ± SEM.

See also Figure S2.

Bassoon Binds Preferentially to SH3I of RBPs

The SH3II domain of RBPs mediates interaction with RIMs (Wang et al., 2000), proteins implied in the recruitment of presynaptic Ca^{2+} channels to release sites (Südhof, 2012). This interaction is mediated by a PXXP motif of RIM (Figure 2A), which can bind to the SH3 domains of RBP1 and RBP2 and contributes to the recruitment of Ca_Vs to the release sites (Kaeser et al., 2011; Wang et al., 2000). To assess if and how RBPs with their three SH3 domains integrates multiple PXXP motif-bearing proteins, we performed quantitative binding assays with purified recombinant proteins utilizing surface plasmon resonance technology. Fragments containing extended SH3I domains of RBP1 or RBP2 and fragments containing the SH3II and SH3III of the RBPs (SH3II+III) exhibited considerable PXXP interactions and thus were used to quantitatively evaluate the binding to immobilized 6xHis-Thioredoxin (His-Trx)-tagged fusion proteins containing PXXP motifs of Bassoon (Bsn12), RIM1, $Ca_V2.1$, and $Ca_V2.2$ (Figure 2E). Bsn12* containing the mutated PXXP motif was immobilized in a control experiment, which resulted in responses not significantly different from background responses induced using immobilized His-Trx control proteins (Figure 2D). We introduced inactivating point mutations into the second, third, or both SH3 domains in the SH3II+III construct to assess

Both EGFP-Bsn10 and EGFP-Bsn10* are localized in cytosolic clusters, when expressed in heterologous cell lines (Figure 2C). mRFP-$Ca_V2.1$ and myc-RBP2 were efficiently recruited into these clusters in cells expressing EGFP-Bsn10, but not those expressing EGFP-Bsn10* (Figure 2C). Importantly, mRFP-$Ca_V2.1$ was only recruited to EGFP-Bsn10, when myc-RBP2 was coexpressed (Figure 2C, middle row). Together these experiments strongly support our notion that RBP might function as a hub linking multiple PXXP motif-containing proteins such as Bassoon and $Ca_V2.1$.

the contribution of SH3II and SH3III to the binding (Figure S2). To correct for different molecular weights of GST-fusion proteins used, molar binding activities (MBAs) were calculated for each interaction pair. The first SH3 domain of both RBPs bound Bsn12 but showed basically no interaction with other PXXP-containing fragments (Figure 2E). Bsn12 bound with comparable strength to SH3II+SH3III, which also interacted with RIM1 and Ca_Vs (Figure 2E). The inactivating mutation of SH3III in the SH3II+SH3III fragment completely prevented binding of Bsn12, whereas Ca_Vs and RIM1 still could bind, though clearly less efficiently in the case of RBP2 (Figure S2). Taking these results together and assuming equimolar ratios of all studied proteins (Holderith et al., 2012), we suggest that Bassoon occupies most likely the first SH3 domain, whereas Ca_Vs and RIM1 may bind to the C-terminal SH3 domains. Thus RBPs can accommodate simultaneous binding of Bassoon and Ca_Vs.

Bassoon Localizes $Ca_V2.1$, but Not $Ca_V2.2$, via Its Interaction with RBP

To test whether Bassoon, RBP, and Ca_Vs can interact in neurons, we performed colocalization and coprecipitation experiments (Figure 3). Multimolecular complexes containing Bassoon, RBP2, and $Ca_V2.1$ were precipitated with specific antibodies against Bassoon and $Ca_V2.1$ from synaptosomal fractions of adult rat brain (Figure 3B) providing evidence for the existence of a tripartite Bassoon-RBP2-$Ca_V2.1$ complex in neurons. Moreover, immunostaining of cultured hippocampal neurons with antibodies against Bassoon, RBP2, and $Ca_V2.1$ or $Ca_V2.2$ revealed colocalization of all three components in individual synapses (Figure 3A). Nearly all RBP2-positive, $Ca_V2.1$-positive, or $Ca_V2.2$-positive synaptic puncta also contained Bassoon immunoreactivity (Figures 3A and 3C; RBP2: 91% ± 1%, Cav2.1: 94% ± 1%, Cav2.2: 93% ± 1%, n = 15 cells from three independent experiments), what is consistent with the presence of Bassoon in most synapses (Altrock et al., 2003). The expression levels of presynaptic proteins vary significantly between individual synapses (Lazarevic et al., 2011). To assess whether synaptic recruitment of Bassoon, RBP2, and Ca_Vs is interdependent, we first compared expression levels of the four proteins at individual synapses by measuring immunofluorescence (IF) intensities for Bassoon, RBP2, $Ca_V2.1$, and $Ca_V2.2$ in presynaptic boutons identified by antisynapsin staining. We calculated Pearson's correlation coefficient (Pearson's r), expressing the degree of linear interdependence of variables, for intensities of Bassoon and Ca_Vs or RBP2 at individual synapses for each cell. Bassoon-$Ca_V2.1$ and Bassoon-RBP2 correlated with remarkably high Pearson's r (0.61 ± 0.03 and 0.65 ± 0.02, respectively) and differed significantly from that of Bassoon-$Ca_V2.2$ (0.32 ± 0.03, n = 10 cells from two independent experiments, $p < 0.001$, ANOVA, Bonferroni posttest; Figure 3D). This illustrates a stronger dependence of RBP2 and $Ca_V2.1$ levels on Bassoon at individual synapses compared to $Ca_V2.2$, which might be due to the Bassoon-dependent recruitment or retention of RBP and $Ca_V2.1$, but not of $Ca_V2.2$, in presynaptic boutons. Thus, coprecipitation of Bassoon, $Ca_V2.1$, and RBP2 from brain tissue and covariance of expression levels of Bassoon, $Ca_V2.1$, and RBP2 strongly suggest that RBP links Bassoon with $Ca_V2.1$ in vivo.

To further explore the possibility that Bassoon controls subcellular localization of Ca_Vs in neurons, we stained for endogenous RBP2, $Ca_V2.1$, and $Ca_V2.2$ in neurons transfected with EGFP-tagged Bassoon (GFP-Bsn). GFP-Bsn localizes to synapses and forms ectopic clusters in the cytoplasm of transfected neurons (Dresbach et al., 2003). We observed robust corecruitment of endogenous RBP2 and $Ca_V2.1$, but not of $Ca_V2.2$, to these cytoplasmic GFP-Bsn clusters (Figure 3E) supporting a role of Bassoon in localizing of $Ca_V2.1$. Overexpressed GFP-Bsn* mutated in the RBP-binding motif fully mirrored the localization of GFP-Bsn in neurons, but completely failed to corecruit both RBP2 and $Ca_V2.1$ (Figure 3E). This suggests that an intact RBP2-interaction interface in Bassoon is necessary for the specific recruitment of P/Q-type channels to the clusters. If Bassoon plays a role in physiological recruitment of $Ca_V2.1$ to synapses, then overexpression of GFP-Bsn should result in an increased recruitment of $Ca_V2.1$ to synaptic sites. To analyze this we calculated Pearson's r for IF intensity of GFP and levels of endogenous RBP2 and $Ca_V2.1$ at individual synapses of neurons expressing GFP-Bsn or GFP-Bsn*. Pearson's r of IF levels for RBP2 and $Ca_V2.1$ were significantly higher in synapses expressing GFP-Bsn compared to synapses expressing GFP-Bsn* (Figures S3A and S3B). This is in line with the proposed role for Bassoon's PXXP motif in mediating the interaction with RBPs. Pearson's r values were lower for immunoreactivity for $Ca_V2.2$ or Piccolo and GFP-Bsn IF levels and did not differ when compared to GFP-Bsn* expressing synapses. This argues for a specific synaptic recruitment of $Ca_V2.1$ and RBP2 by overexpressed Bassoon and suggests that Bassoon controls synaptic localization of RBP2 and $Ca_V2.1$ in neurons by mechanisms requiring the intact PXXP motif that mediates its interaction with RBPs.

Bassoon Is Required for Normal Recruitment of $Ca_V2.1$ to Synapses

To confirm the preference of Bassoon for $Ca_V2.1$ over $Ca_V2.2$ apparent from specific recruitment of $Ca_V2.1$ in GFP-Bsn expressing neurons and to further assess the role of Bassoon in the synaptic localization of RBP2 and $Ca_V2.1$, we analyzed the effect of Bassoon deletion on synaptic localization of these proteins. To this end, we prepared dissociated hippocampal cultures, where neurons from *Bsn*-deficient ($Bsn^{-/-}$) mice (Hallermann et al., 2010) and their wild-type (WT) siblings were coplated in a 1:1 ratio and grown for 23 days in vitro (DIV). The cultures were immunostained with specific antibodies, IF levels of RBP2, Ca_Vs, and synaptophysin were measured at individual synapses defined by synapsin staining and compared in Bassoon-containing versus Bassoon-lacking synaptic boutons (Figures 4A and 4B). As Bassoon can be detected in >90% of synapses of WT neurons (Lazarevic et al., 2011) staining against Bassoon is a reliable way to discriminate between synapses formed by neurons from WT and from $Bsn^{-/-}$ animals. We found a significant reduction of immunoreactivity for RBP2 (0.84 ± 0.03 in $Bsn^{-/-}$ versus 1 ± 0.03 WT, values normalized to WT cells; n = 18 cells, $p < 0.0001$, two-tailed t test, four independent experiments) and for $Ca_V2.1$ (0.71 ± 0.03 versus 1 ± 0.05, n = 18, $p < 0.0001$) at synapses of $Bsn^{-/-}$ neurons. No significant decrease was detected for immunostaining intensity of $Ca_V2.2$ (0.93 ± 0.04 versus 1 ± 0.06; n = 18, p = 0.32) or synaptophysin

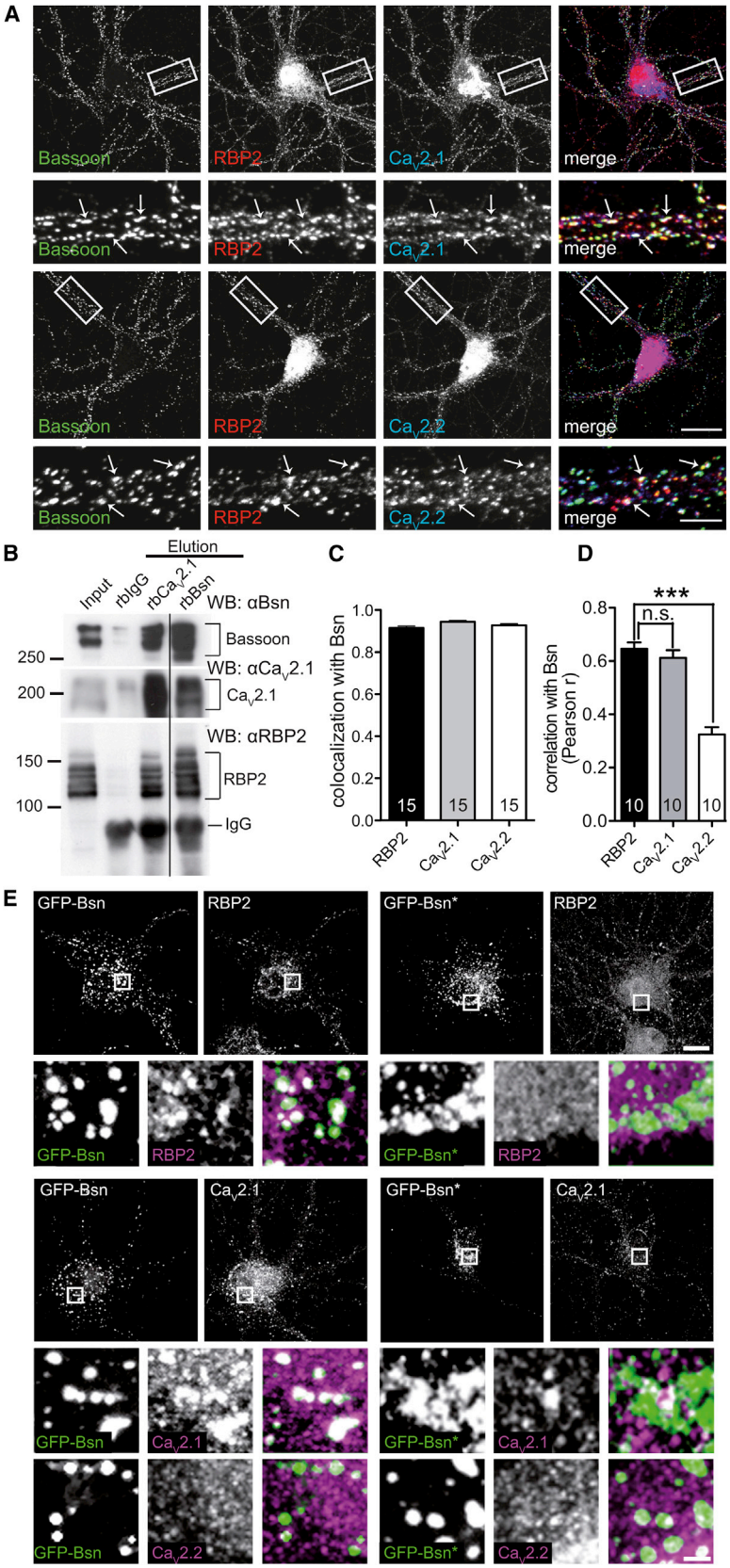

Figure 3. Bassoon Is Linked to $Ca_V2.1$, but Not $Ca_V2.2$, via Interaction with RBP

(A) Staining of hippocampal neurons (DIV21) with antibodies against Bassoon, RBP2, $Ca_V2.1$, and $Ca_V2.2$ (grayscale images) demonstrates their colocalization (colored overlay images; arrows) in individual synapses. The color code corresponds to lettering in grayscale image. Regions shown in high magnification are boxed. Scale bars represent 20 μm in overview and 5 μm in insets.

(B) Protein complexes containing Bassoon, RBP2, and $Ca_V2.1$ were isolated from brain synaptosomal fractions with antibodies against Bassoon and $Ca_V2.1$, but not with control rabbit IgGs. Position of bands corresponding to proteins of interest are indicated.

(C) Quantification of colocalization of Bassoon in synaptic puncta immunoreactive for RBP, $Ca_V2.1$, and $Ca_V2.2$. Bars show mean ± SEM. Values in bars indicate number of analyzed cells.

(D) Correlation of IF intensity for RBP2, $Ca_V2.1$, and $Ca_V2.2$ with Bassoon at individual synapsin-positive presynapses. Bars show mean ± SEM; ***$p < 0.001$, n.s. $p > 0.05$. Values in bars indicate number of analyzed cells.

(E) Cytoplasmic clusters formed by overexpressed GFP-Bsn recruit endogenous RBP2, $Ca_V2.1$, but not $Ca_V2.2$. This recruitment depends on the presence of an intact RBP-binding site on Bassoon and does not occur with RBP-binding-deficient GFP-Bsn*. Large images show overviews of neurons overexpressing GFP-Bsn and their counterstains with antibodies against RBP2 or $Ca_V2.1$. Higher magnification of cytoplasmic GFP-Bsn clusters formed in transfected neurons are boxed. The color images display overlays of GFP-fluorescence (green) and immunostaining (magenta) for proteins of interest. Corecruitment with GFP-Bsn is observed for RBP2 and $Ca_V2.1$, but not for $Ca_V2.2$. Scale bars represent 20 μm in overview and 5 μm in insets. See Figure S3 for enrichment of RBP2 and Cav2.1 in synapses overexpressing GFP-Bsn.

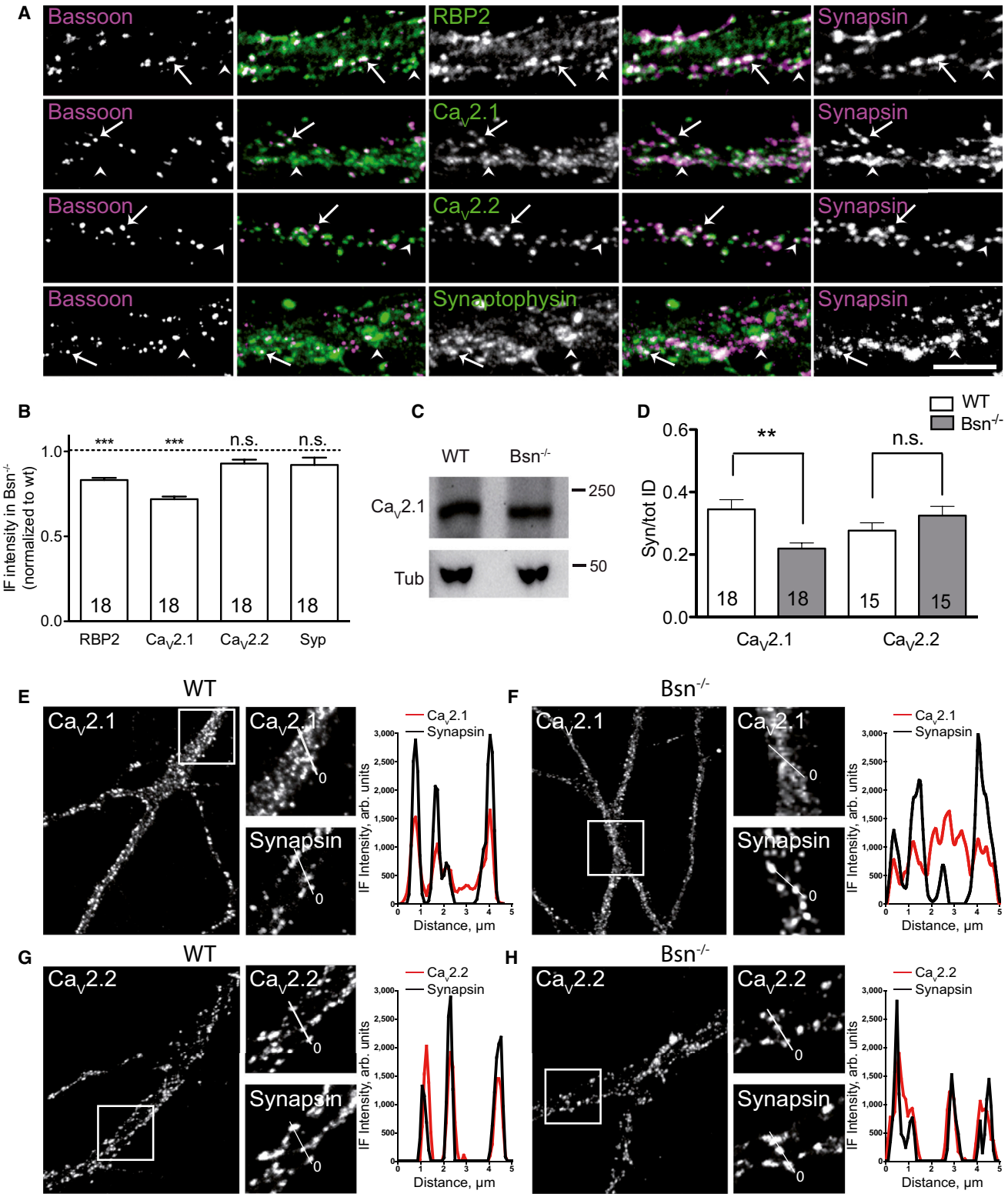

Figure 4. Bassoon Regulates Synaptic Recruitment of RBP2 and $Ca_V2.1$ Without Affecting $Ca_V2.2$

(A) Staining of mixed neuronal cultures from *Bsn*$^{-/-}$ and WT mice with antibodies against Bassoon, synapsin, and RBP2 (1st row) or $Ca_V2.1$ (2nd row), $Ca_V2.2$ (3rd row), or synaptophysin (4th row). Arrows mark Bassoon-containing, arrowheads Bassoon-deficient synapses. The second and fourth images in each row show overlays of images to their left and right. Scale bar represents 10 µm.

(legend continued on next page)

(0.92 ± 0.06 versus 100 ± 5, n = 18, p = 0.38). The decrease of RBP2 and $Ca_V2.1$, but not of $Ca_V2.2$ or synaptophysin was also observed when *Bsn*$^{-/-}$ and WT neurons were plated separately and grown in parallel (data not shown). Thus, lack of Bassoon expression affects specifically the presynaptic localization of RBP2 and $Ca_V2.1$, but not that of $Ca_V2.2$.

Decreased levels of $Ca_V2.1$ in Bassoon-lacking synapses might be due either to a defect in their synaptic localization or to disturbed regulation of the expression of these channels. The expression levels of $Ca_V2.1$ were similar in cell lysates prepared form mature cultured hippocampal neurons from WT or *Bsn*$^{-/-}$ animals as assessed by immunoblot analysis (Figure 4C). To explore the possibility of perturbed synaptic recruitment in absence of Bassoon, we examined the distribution of $Ca_V2.1$ and $Ca_V2.2$ between synapses and extrasynaptic (surface and intracellular) membranous compartments in neurons from *Bsn*$^{-/-}$ and WT mice. To this end, we stained hippocampal neurons with antibody against Ca_Vs and synapsin (to define synaptic boutons) and measured IF intensities of Ca_Vs staining either in the mask formed by synaptic marker (syn) or in whole images (total staining, tot). The total intensity of IF for the channels did not differ in *Bsn*$^{-/-}$ and WT cells confirming the immunoblot results. However, the syn/tot ratio was significantly lower in Bassoon-lacking as compared to WT neurons for $Ca_V2.1$ (0.22 ± 0.02 in *Bsn*$^{-/-}$ versus 0.35 ± 0.03 in WT, n = 18, p = 0.001, two-tailed t test, three independent cultures; Figures 4D–4F). In contrast, the ratio did not differ significantly for $Ca_V2.2$ (0.32 ± 0.03 versus 0.28 ± 0.02, n = 15, p = 0.224; Figures 4D, 4G, and 4H). Moreover, an inspection of the distribution of staining in *Bsn*$^{-/-}$ and WT neurons showed a clearly increased extrasynaptic IF for $Ca_V2.1$ in *Bsn*$^{-/-}$ neurons, while only low extrasynaptic $Ca_V2.1$-IF was detected in WT neurons (IF intensity line scans in Figures 4E–4H). These results imply that lack of Bassoon leads to specific deficits in the localization of RBP2 and $Ca_V2.1$ to presynapses.

Acute Interference with Bassoon-RBP Interaction Affects Synaptic Localization of $Ca_V2.1$ and Weakens Synaptic Transmission

The reduction of synaptic levels of RBP2 and $Ca_V2.1$ might also be a consequence of adaptive processes during development induced by Bassoon deficiency in *Bsn*$^{-/-}$ neurons. To exclude this possibility, we acutely interfered with Bassoon-RBP2 interaction in mature neurons (DIV23) prepared from newborn *Bsn*$^{-/-}$ mice and their WT siblings by means of 2 hr application of 1 μM TAT-conjugated peptides mimicking either the RBP-binding site on Bassoon sequence (aa 2,880–2,899; TAT-WT) or containing the above-described 3 aa mutation in the RBP-binding site (TAT-RBM). TAT-WT, but not TAT-RBM peptide, efficiently interfered with Bassoon-RBP2 binding in an in vitro competition assay (Figure 5A) and did not significantly affect basic membrane properties of cultured hippocampal neurons (Figure S4). A slight change is observed for the half-width of action potentials what may indicate an effect of the TAT peptides on presynaptic Ca^{2+} influx, however, neither TAT-RBM nor TAT-WT cause significant differences from controls (Figure S4E). The effect of TAT-peptides on the synaptic recruitment of RBP2 and $Ca_V2.1$ via Bassoon was assessed by measuring IF levels at individual synapses as described above. Treatment with TAT-WT, but not with TAT-RBM, induced a significant acute reduction of RBP2 and $Ca_V2.1$ levels in neurons from WT mice (RBP2: 0.77 ± 0.05 versus 1 ± 0.05, TAT-WT versus TAT-RBM, n = 19 versus 18 cells, p < 0.001, ANOVA with Bonferroni posttest, three independent experiments; $Ca_V2.1$: 0.69 ± 0.05 versus 1 ± 0.05, n = 24 versus 23, p < 0.001; Figures 5B–5D). The same treatment had no effect on synaptic localization of $Ca_V2.2$ (0.94 ± 0.08 versus 1 ± 0.06, n = 16 versus 19, p > 0.05; Figure 5E). A similar effect was seen after treatment of neurons derived from embryonic rats (data not shown). Importantly, the application of the TAT-WT had no effect on synaptic levels of RBP2 or Ca_Vs in the neurons from *Bsn*$^{-/-}$ mice (RBP2: 0.71 ± 0.06 versus 0.67 ± 0.05, TAT-WT versus TAT-RBM, normalized to respective IF in WT cultures, n = 20 versus 20, p > 0.05, ANOVA with Bonferroni posttest; $Ca_V2.1$: 0.48 ± 0.04 versus 0.52 ± 0.04, n = 25 versus 24, p > 0.05; $Ca_V2.2$: 1.15 ± 0.1 versus 0.99 ± 0.06, n = 15 versus 24, p > 0.05; Figures 5B–5E). This indicates that the effect of TAT-WT is exclusively dependent on Bassoon and not due to interference with the interaction of the SH3 domain of RBP with RIM or Ca_Vs.

Having shown the specificity of TAT peptides for Bassoon-dependent recruitment of Ca_Vs, we used them to test the role of the Bassoon PXXP motif in synaptic transmission. To this end, we applied the TAT-WT and TAT-RBM peptides to acute hippocampal slices and recorded field excitatory postsynaptic potentials (fEPSP) in the stratum radiatum of the hippocampal CA1 region evoked by Schaffer collateral stimulation (Figure 5F). At these synapses, transmission relies predominantly on Ca^{2+} influx through $Ca_V2.1$ and $Ca_V2.2$, which (Luebke et al., 1993; Wu and Saggau, 1994). We observed a significant reduction of normalized fEPSP slopes in slices treated with TAT-WT compared to those treated with TAT-RBM (48.1% ± 11.8% of TAT-RBM, n = 8, p = 0.0032; Figures 5G and 5H). Importantly, a comparable reduction of synaptic transmission by TAT-WT peptide was also seen upon pharmacological isolation of $Ca_V2.1$-driven transmission using the specific blocker of $Ca_V2.2$ ω-conotoxin GVIA (Cono, 45.2% ± 5.8% of TAT-RBM,

(B) Quantification of IF intensities in *Bsn*$^{-/-}$ synapses normalized to mean IF of WT synapses. Note selective reduction of synaptic RBP2 and $Ca_V2.1$ levels in *Bsn*$^{-/-}$.

(C) $Ca_V2.1$ expression in WT and *Bsn*$^{-/-}$ mature (23 DIV) hippocampal cell lysate.

(D) Quantification of relative synaptic pool of Ca_Vs measured as mean synaptic IF normalized to total IF measured along neurites of WT and Bsn$^{-/-}$ cells. In both plots (B and D) bars show mean ± SEM; ***p < 0.001; **p = 0.001; n.s. = p > 0.05. Values in bars indicate number of analyzed cells.

(E–H) Example images displaying the distribution of $Ca_V2.1$ (E and F) and $Ca_V2.2$ (G and H) in neurons from WT (E and G) and *Bsn*$^{-/-}$ (F and H) mice. Line scans provide IF intensity for Ca_Vs (red) and synapsin (black) along the line shown in the insets. Note the higher confinement of immunoreactivity for $Ca_V2.1$ to synapses in WT than in *Bsn*$^{-/-}$ neurons. The distribution of $Ca_V2.2$ is not affected by Bassoon deficiency. Scale bars represent 10 μm in overview and 2.5 μm in insets. See also Figure S3.

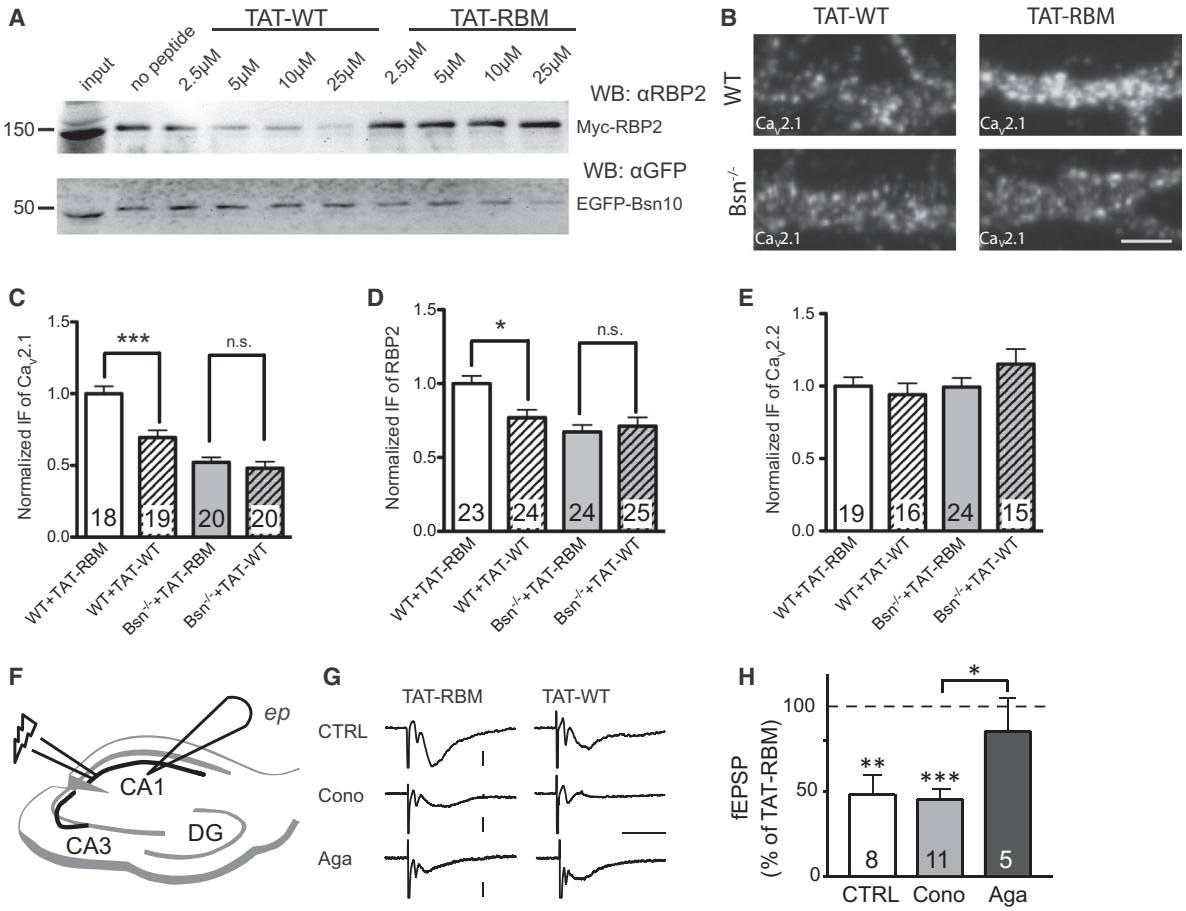

Figure 5. Interference with Bassoon-RBP Interaction Impairs Synaptic Localization of $Ca_V2.1$ and Diminishes $Ca_V2.1$-Mediated Synaptic Transmission

(A) Lysates from cells expressing myc-RBP2 and EGFP-Bsn10 fragments were incubated with increasing concentrations of TAT-WT or TAT-RBM control peptides before coprecipitation. EGFP-Bsn10 was successfully precipitated in all samples. Increasing concentrations of TAT-WT peptide interfered with the coprecipitation of Myc-RBP2, whereas the TAT-RBM had no effect. Positions of bands corresponding to proteins of interest are indicated.

(B–E) Treatment of neurons with TAT-WT peptide leads to reduction of $Ca_V2.1$ (B and C) and RBP2 (D) IF levels at WT but not $Bsn^{-/-}$ synapses. (E) $Ca_V2.2$ levels are unaffected. (B) Example stains for $Ca_V2.1$ in WT and $Bsn^{-/-}$ neurons treated with TAT-WT and TAT-RBM. Scale bar represents 5 μm. Quantification of IF intensities for $Ca_V2.1$, RBP2, and $Ca_V2.2$ at individual synapses of WT and $Bsn^{-/-}$ neurons treated with either peptide and normalized to IF in WT cultures treated with the control peptide is shown in (C–E).

(F) fEPSPs were recorded from the stratum radiatum of the hippocampal CA1 region upon Schaffer collateral stimulation.

(G) Sample average traces from slices incubated with TAT-WT or TAT-RBM peptides without inhibitors (CTRL) or in the presence of ω-conotoxin GVIA (Cono) or ω-agatoxin IVA (Aga). Vertical scale bar from top to bottom 0.4, 0.4, and 0.2 mV, horizontal 10 ms.

(H) fEPSPs were significantly reduced upon TAT-WT incubation without toxins and upon isolation of $Ca_V2.1$ driven-transmission using conotoxin, but not if transmission relied primarily on $Ca_V2.2$ in the presence of agatoxin. Values were normalized to transmission in slices incubated with control peptides. In all plots, ***$p < 0.001$; **$p < 0.01$; *$p < 0.05$; n.s. = $p > 0.05$. Values in bars indicate number of cells or slices analyzed.

See also Figure S4.

$n = 11$, $p < 0.001$; Figures 5G and 5H). This suggested that transmission relying on Ca^{2+} influx through $Ca_V2.1$ is affected. In contrast, the transmission component dependent on $Ca_V2.2$ (isolated by ω-agatoxin IVA, Aga) was similar in TAT-WT- and TAT-RBM-treated slices. As $Ca_V2.1$ and $Ca_V2.2$ do not contribute to dendritic signaling in CA1 pyramids (Higley and Sabatini, 2008), changes in release efficiency explain this data most plausibly. Again, this pointed to the specific regulation of $Ca_V2.1$-dependent transmission by the Bassoon-RBP interaction (85.2% ± 20.7%, $n = 5$, $p = 0.51$, Aga versus Cono: $p = 0.025$; Figure 5H).

Bassoon Controls via Its Interaction with RBP Specifically the Contribution of $Ca_V2.1$ to Synaptic Vesicle Exocytosis

To investigate the effect of aberrant localization of RBP2 and $Ca_V2.1$ in $Bsn^{-/-}$ synapses on synaptic vesicle exocytosis, we first visualized efficiency of synaptic vesicle recycling in individual synapses by means of uptake of anti-synaptotagmin-1 antibody (Stg1Ab) in living neurons (Kraszewski et al., 1995; Lazarevic et al., 2011). This antibody recognizes the lumenal domain of synaptotagmin-1 and, if applied to media, gets internalized during vesicle recycling that follows each fusion event. Using

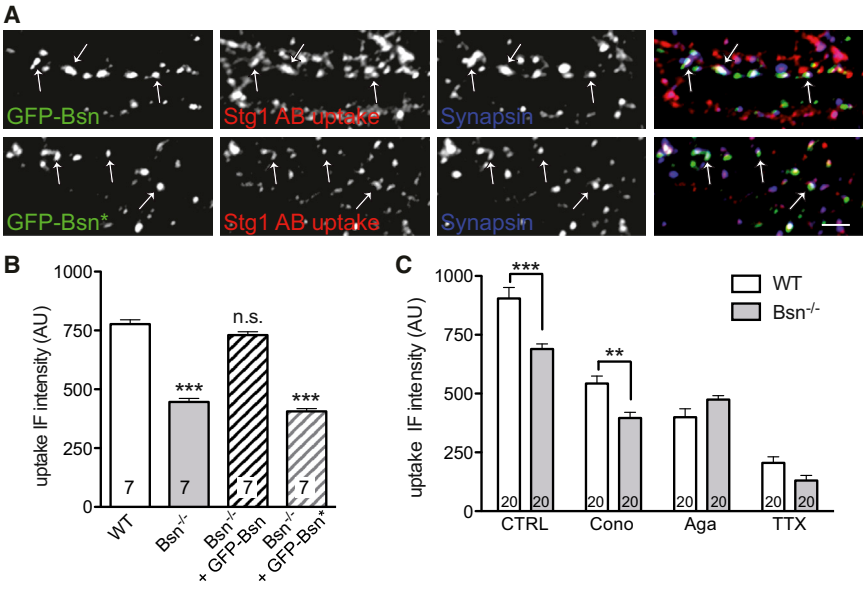

Figure 6. Vesicle Recycling Mediated by $Ca_V2.1$ Depends on Bassoon-RBP Binding

(A) GFP-Bsn and GFP-Bsn* do not differ in their synaptic targeting in $Bsn^{-/-}$ neurons. Arrows show synapses of neurons expressing GFP fusion protein. Uptake of synaptotagmin luminal antibodies (Stg1 AB) is detected. Scale bar represents 2.5 μm.

(B) Stg1Ab-uptake is reduced in $Bsn^{-/-}$ compared to WT synapses and can be rescued in synapses expressing Bsn-GFP, but not in cells expressing GFP-Bsn*.

(C) Quantification of Stg1Ab-uptake in cultures from $Bsn^{-/-}$ and WT mice without toxin treatment or after ω-conotoxin GVIA (Cono), ω-agatoxin IVA (Aga), or tetrodotoxin (TTX) application. Values were normalized to uptake in nontreated WT cultures. In all plots bars show mean ± SEM; ***$p < 0.001$; **$p < 0.01$; *$p < 0.05$; n.s. = $p > 0.05$. Values in bars indicate number of cells analyzed.

See also Figure S5.

this technique the pool of vesicles exocytosed during a period of time can be measured as fluorescence intensity of antibody taken up. The endogenous network activity-driven Stg1Ab uptake was significantly lower in $Bsn^{-/-}$ neurons than in WT neurons (CTRL: 446 ± 15 versus 777 ± 19 AU, $Bsn^{-/-}$ versus WT, n = 7 cells; $p < 0.001$, one-way ANOVA with Bonferroni posttest; replicated in two independent experiments; Figures 6A–6C and S5A). This defect was not due to the changes in network activity in the absence of Bassoon and was fully dependent on cell-autonomous functions of Bassoon as transfection of scattered single neurons in culture from $Bsn^{-/-}$ animals with GFP-Bsn completely rescued vesicle recycling (730 ± 14 AU; Figures 6A and 6B). Importantly, expression of recombinant GFP-Bsn*, bearing the mutated RBP-binding PXXP motif, could not rescue the recycling defect and was statistically not different from nontransfected $Bsn^{-/-}$ neurons (407 ± 12 AU; Figures 6A and 6B). This strongly supports our notion that Bassoon controls neurotransmitter release via its RBP-mediated recruitment of Ca_Vs to release sites.

To assess whether specific decrease in synaptic levels of $Ca_V2.1$ in Bassoon-lacking neurons lead to a decrease in $Ca_V2.1$-driven exocytosis of synaptic vesicles, we quantified Stg1Ab uptake upon pharmacological block of $Ca_V2.1$ or $Ca_V2.2$ using specific toxins. The Stg1Ab uptake in neurons treated with $Ca_V2.2$ blocker ω-conotoxin GVIA resulting in merely $Ca_V2.1$-dependent neurotransmission was significantly lower in $Bsn^{-/-}$ neurons compared to WT (CTRL: 689 ± 22 versus 904 ± 47 AU, $Bsn^{-/-}$ versus WT, n = 20 cells; $p < 0.001$, Cono: 396 ± 24 versus 543 ± 31, n = 20, $p < 0.01$; one-way ANOVA with Bonferroni posttest, two independent experiments; Figures 6C and S5B). In contrast, the uptake in neurons treated with ω-agatoxin IVA that blocks specifically $Ca_V2.1$ did not differ significantly (Aga: 475 ± 17 versus 400 ± 36, n = 20, $p > 0.05$; TTX: 130 ± 22 versus 205 ± 26 WT, n = 20, $p > 0.05$; Figures S5C and S5D). This implies that release driven by Ca^{2+} influx through $Ca_V2.1$ is strongly reduced in absence of Bassoon, whereas $Ca_V2.2$-driven release stays unaffected. This supports the view of an important role of Bassoon in the functional recruitment of $Ca_V2.1$ into presynaptic release sites.

Synaptic Transmission Relies More on $Ca_V2.2$ upon Bassoon Deletion

To test whether the aberrant synaptic localization of $Ca_V2.1$ in $Bsn^{-/-}$ neurons alters the synaptic transmission properties, we performed patch-clamp recordings from cultured hippocampal neurons from $Bsn^{-/-}$ and WT mice. We observed a significant decrease of spontaneous mEPSC frequency in $Bsn^{-/-}$ neurons (interevent interval: 145 ± 26 versus 476 ± 80 ms, WT versus $Bsn^{-/-}$, n = 8 versus 11, $p < 0.0001$, Kolmogorov-Smirnov test; Figure 7A). This might be due to a reduction either in the number of synapses or in synaptic release probability in $Bsn^{-/-}$ mice. To test this we calculated the density of excitatory synapses on 20 μm long proximal (10–30 μm from the cell body) and distal dendritic segments (60–80 μm) in neurons stained with antibodies against synapsin, vGLUT, and homer. No significant differences were observed (proximal dendrites: 2.2 ± 0.1 versus 2.1 ± 0.1; distal: 2.4 ± 0.1 versus 2.3 ± 0 synapses/10 μm, WT versus $Bsn^{-/-}$, n = 7 cells each). This suggests that the observed reduction in the spontaneous mEPSC frequency in $Bsn^{-/-}$ likely reflects lower synaptic release probability, what is consistent with reduced Stg1Ab uptake observed in these cultures. The amplitudes of mEPSC were not changed significantly (15.4 ± 1.2 versus 13.3 ± 1.0 pA, WT versus $Bsn^{-/-}$, n = 8 and 11 animals, p = 0.081, Kolmogorov-Smirnov test; Figure 7B), however, their kinetic properties differed slightly (Figures 7B, inset, and S6A). This might reflect modifications in the postsynaptic receptor apparatus of cultured $Bsn^{-/-}$ neurons as reported previously (Ghiglieri et al., 2009).

Next, we assessed whether the Bassoon deletion affects the relative contribution of $Ca_V2.1$ and $Ca_V2.2$ to evoked synaptic transmission in the same preparation. We measured transmission between paired cells before and after applying specific

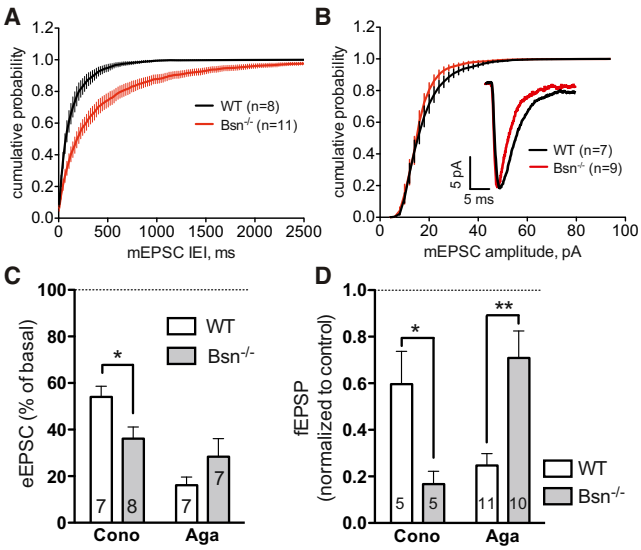

Figure 7. Reduced Contribution of $Ca_V2.1$ to Synaptic Transmission in $Bsn^{-/-}$ Mice

(A and B) Analysis of spontaneous neurotransmission in cultures from $Bsn^{-/-}$ and WT neurons. Cumulative distributions (mean values ± SEM) are plotted for interevent intervals (IEI) (A) and amplitudes (B) of mEPSC.

(C) Quantification of evoked EPSCs before toxin addition and after subsequent treatment of WT or $Bsn^{-/-}$ neurons with ω-conotoxin GVIA (Cono) or ω-agatoxin IVA (Aga) or vice versa. eEPSCs amplitudes were normalized for each cell to the response before addition of toxins. Note the higher sensitivity to conotoxin and the lower sensitivity to agatoxin in $Bsn^{-/-}$ cultures (see also Figure S6B).

(D) fEPSPs evoked by Schaffer collateral stimulation and recorded from the stratum radiatum of the CA1 region were significantly reduced upon conotoxin but increased upon agatoxin treatment in slices from $Bsn^{-/-}$ mice compared to their WT siblings, suggesting a decrease in $Ca_V2.1$-driven and enhanced contribution of $Ca_V2.2$ to synaptic transmission. Values were normalized to fEPSPs measured in slices without toxin treatment on the same day (dashed line). Values in bars indicate number of cells and slices analyzed. Bars represent mean ± SEM in all plots; $^{**}p < 0.01$; $^{*}p < 0.05$.

channel blockers and calculated the toxin-induced inhibition of transmission relative to initial transmission. Relative measurements appeared more appropriate to us, considering high variability of coupling of individual neurons in dense mature (DIV 14–21) mass cultures used here. The blockage of $Ca_V2.2$ using ω-conotoxin GVIA revealed a significantly lower proportion of transmission mediated by $Ca_V2.1$ in $Bsn^{-/-}$ neurons compared with WT controls (36% ± 5% versus 54% ± 5% of transmission before toxin addition, $Bsn^{-/-}$ versus WT, p = 0.0218, two-tailed t test; Figures 7C and S6B). The proportional transmission in the presence of ω-agatoxin IVA, (mediated by $Ca_V2.2$) was also slightly increased in absence of Bassoon (28% ± 8% versus 16% ± 4%, p = 0.17, two-tailed t test; Figure 7C).

To extrapolate the data obtained from cultured cells to organized brain tissue, we recorded field excitatory postsynaptic potentials (fEPSP) in the stratum radiatum of the hippocampal CA1 region evoked by Schaffer collateral stimulation in acute slices from $Bsn^{-/-}$ and WT mice. In line with previous data (Sgobio et al., 2010), the normalized fEPSP slope did not differ between slices from $Bsn^{-/-}$ and WT littermates (WT versus $Bsn^{-/-}$: 1.11 ± 0.16 versus 1.14 ± 0.17 ms^{-1}, n = 17 versus 14 animals, p = 0.915, two-population t test). However, we measured significantly decreased fEPSPs upon isolation of ω-conotoxin GVIA-resistant, $Ca_V2.1$-driven transmission in $Bsn^{-/-}$ compared to WT (WT versus $Bsn^{-/-}$: 0.60 ± 0.14 versus 0.17 ± 0.05 normalized to fEPSPs of nontreated slices of either genotype, n = 5 versus 5, p = 0.035; Figure 7D). In contrast, the ω-agatoxin IVA-resistant transmission, relying on $Ca_V2.2$, was significantly higher in $Bsn^{-/-}$ mice (WT versus $Bsn^{-/-}$: 0.25 ± 0.05 versus 0.71 ± 0.12, n = 11 versus 10, p = 0.003; Figures 7D and S6C) suggesting enhanced involvement of $Ca_V2.2$ in synaptic transmission in $Bsn^{-/-}$ animals. In summary, these results strongly imply an important role of Bassoon specifically controlling contribution of $Ca_V2.1$ to synaptic transmission. Moreover, they suggest enhanced compensatory recruitment of $Ca_V2.2$ in $Bsn^{-/-}$ animals leading to a recovery of evoked transmission at Schaffer collaterals-CA1 synapses.

DISCUSSION

Here, we describe RBPs as a binding partner of Bassoon. This interaction links Bassoon physically to RBP-interacting presynaptic Ca_Vs and functions in the specific recruitment of $Ca_V2.1$-containing P/Q-type channels to active zones. Consistently, we observed a decrease of $Ca_V2.1$ and RBP2 at synapses of $Bsn^{-/-}$ neurons associated with a reduced $Ca_V2.1$-driven synaptic vesicle exocytosis and $Ca_V2.1$-driven transmission in hippocampal primary cultures and slices from $Bsn^{-/-}$ animals. These findings place Bassoon as a new player in the complex molecular machinery that controls coupling of Ca_Vs to transmitter release sites. Unlike the previously known Ca_V regulators, which equally control both N- and P/Q-type channels (Gundelfinger and Fejtova, 2012; Inchauspe et al., 2004; Kaeser et al., 2011; Südhof, 2012), Bassoon functions specifically in the recruitment of $Ca_V2.1$ to tune the exact arrangement of presynaptic release sites.

Bassoon Is a Component of the RBP-Based Protein Complex Organizing Ca_Vs at Vesicular Release Sites

Various protein-protein binding assays identified the interaction of an PXXP motif in the C-terminal part of Bassoon with SH3 domains of RBPs. RBPs are evolutionary conserved proteins bearing three SH3 domains, which can interact with multiple partners including RIMs and α-subunits of L-type, P/Q-type, and N-type Ca^{2+} channels (Hibino et al., 2002; Kaeser et al., 2011; Wang et al., 2000). Quantitative in vitro binding assays comparing the binding of RBPs to their presynaptically localized interaction partners revealed Bassoon as the virtually exclusive binding partner of the first SH3 domain, whereas RIM1 and $Ca_V2.1$, as well as $Ca_V2.2$, bound second and third domain. Thus, RBPs can function as a molecular hub integrating binding of Bassoon, RIMs, and Ca_Vs to spatially and functionally couple presynaptic Ca_Vs to the CAZ surrounding docking and fusion sites for SVs. The functional properties of presynapses including their release probability or contribution of N- and P/Q-type current to the release are highly variable between different cell types and even along single axons (Ariel et al., 2012; Murthy et al., 1997). Expression of RIMs and RBPs occurs from multiple genes

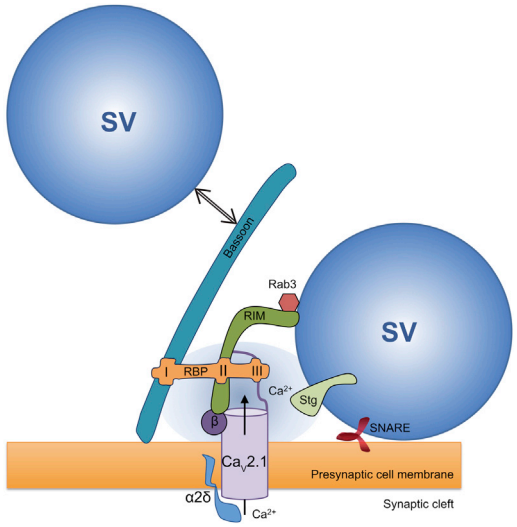

Figure 8. RBP-Based Multiprotein Complex Organizes Presynaptic Release Sites

The CAZ proteins RIM, RBP, and Bassoon and the auxiliary subunits of Ca_Vs, α2δ, and β control synaptic localization of Ca_Vs (Gundelfinger and Fejtova, 2012). RBPs link via their SH3 domains-mediated interactions Bassoon, RIM, and Ca_Vs to achieve efficient positional priming of synaptic vesicles (SV). Bassoon is necessary for rapid replenishment of the release sites (Hallermann et al., 2010) likely by SV tethering to active zones. RIM binds SV-associated Rab3 (Südhof, 2012). Thus, the RBP-based multiprotein complex organizes release sites by spatial and functional coupling of multiple steps of the SV cycle.

and involves complex splicing (Kaeser et al., 2008; Mittelstaedt and Schoch, 2007; Wang and Südhof, 2003). It will be interesting to investigate how the molecular diversity of RBP-based multiprotein complexes contributes to this functional variability. Serine-2893 included in the RBP-binding PXXP motif of Bassoon is phosphorylated in vivo (Collins et al., 2005; Munton et al., 2007). Phosphorylation of PXXP motifs can influence their binding to SH3 domains (Anggono et al., 2006). Accordingly, phosphorylation of S2893 in Bassoon might represent a mechanism of fast modulation of coupling of $Ca_V2.1$ to vesicular release sites. While exclusive synaptic recruitment of $Ca_V2.1$ (but not $Ca_V2.2$) by Bassoon in neurons was apparent throughout this study, the molecular mechanism of this specificity is unclear so far. The in vitro binding assay did not show any clear preference of binding neither of Bassoon nor Ca_Vs to one RBP isoform, suggesting that more complex regulation takes place. A recent proteomic study supported a preferential association of Bassoon with $Ca_V2.1$-containing channels (Müller et al., 2010). Future comparative analysis of molecular composition of $Ca_V2.1$- and $Ca_V2.2$-containing complexes should help to tackle this question.

Recruitment of Ca_Vs to Vesicular Release Sites at CNS Synapses

To date, active zone scaffolding proteins RIMs and RBPs have been implicated in organizing vesicular release sites by molecular linkage of Ca^{2+} channels, components of the release machinery and synaptic vesicles (Kaeser et al., 2011; Kiyonaka et al., 2007; Liu et al., 2011; Wang et al., 2000) (Figure 8). *Drosophila* RBP (DRBP) links Ca_Vs to Bruchpilot (BRP), the main presynaptic scaffolding protein at larval neuromuscular junctions. Loss of DRBP leads to reduction of presynaptic Ca_V density and basically abolishes evoked neurotransmission (Liu et al., 2011). A deletion phenotype of RBPs is unknown in mammals, but it was suggested that RBPs link Ca_Vs to release sites via their interaction with RIMs, which in addition regulates Ca_Vs by a direct interaction (Hibino et al., 2002; Kaeser et al., 2011; Wang et al., 2000). However, expression of a RIM deletion construct in RIM1/2-deficient cells, which restores normal priming but leaves RIM-dependent Ca_V recruitment impaired, had milder effects on evoked synaptic transmission compared to severe defects in DRBP null mutants (Kaeser et al., 2011; Liu et al., 2011). Similarly, in absence of Bassoon total transmission is only slightly affected (also due to compensation through increased $Ca_V2.2$ as discussed later) but contribution of both channels to transmission differs significantly. We observed an ~30% reduction of synaptic localization of $Ca_V2.1$ in $Bsn^{-/-}$ synapses, what is comparable with the reduction seen in full *RIM1/2* knockout (i.e., 40%) (Kaeser et al., 2011) or in *Drosophila* mutants for DRBP (25%) (Liu et al., 2011), DRIM (30%–40%) (Graf et al., 2012) or Bruchpilot (40%) (Kittel et al., 2006). These rather mild effects on Ca_V localization are likely due to multiple interactions coregulating the synaptic recruitment and coupling of Ca_Vs (Figure 8). CAZ proteins likely mediate the exact positioning of Ca_Vs relative to release sites, whereas the auxiliary channel subunits β and α2δ regulate the synaptic abundance of Ca_Vs mainly by controlling their trafficking to axons (Hoppa et al., 2012; Kiyonaka et al., 2007). The observed redistribution of $Ca_V2.1$ from synaptic to extrasynaptic pools in the absence of functional Bassoon-RBP interaction suggests that Bassoon acts probably in recruiting/retention of axonal $Ca_V2.1$ at synaptic release sites. Additional factors regulating presynaptic availability of Ca_Vs might be neurexins and their interaction with postsynaptic neuroligins (Missler et al., 2003). Altogether, multiple targeting mechanisms coexist to assure proper synaptic localization and function of presynaptic Ca_Vs offering variable modes of regulation to control the release properties at individual synaptic boutons along axons.

Specific Recruitment of $Ca_V2.1$ by Bassoon

Removal of RIMs or β and α2δ auxiliary subunits leads to a decrease in total Ca^{2+} influx without altering the relative contribution of N- and P/Q-currents to synaptic transmission (Han et al., 2011; Hoppa et al., 2012) implying a role for these proteins in nonselective synaptic recruitment of presynaptic Ca_Vs. In contrast, Bassoon mediates specific recruitment of $Ca_V2.1$ to synaptic sites. Consequently, as shown here, in the absence of Bassoon function or acute interference with Bassoon-RBP interaction the relative contribution of $Ca_V2.1$ to synaptic transmission is decreased. Strikingly, while the total transmission was reduced due to reduction of the $Ca_V2.1$-driven release upon the acute interference with RBP-Bassoon binding, this decrease was essentially compensated by increased functional recruitment of $Ca_V2.2$ in mutant animals. This implies that vesicular release sites normally coupled to $Ca_V2.1$ may switch to $Ca_V2.2$ if Bassoon-RBP interaction is disrupted during ontogenesis.

This is consistent with the previous observation that $Ca_V2.2$ can functionally replace $Ca_V2.1$ (Cao and Tsien, 2010; Jun et al., 1999). It has been proposed that synapses possess Ca_V slots of two types: $Ca_V2.1$ rejecting (occupied only by $Ca_V2.2$) and $Ca_V2.1$ nonrejecting (occupied preferentially by $Ca_V2.1$) (Cao et al., 2004; Cao and Tsien, 2010). We propose that Bassoon specifies the $Ca_V2.1$ nonrejecting slots, whereas RIMs and β and α2δ auxiliary subunits associate with all slots. The contribution of N-type and P/Q-type currents to synaptic transmission differs among brain synapses (Iwasaki et al., 2000) and is regulated during development (Fedchyshyn and Wang, 2005; Scholz and Miller, 1995) and processes of synaptic plasticity (Ahmed and Siegelbaum, 2009). A differential recruitment of specific channel types to release sites influences presynaptic release probability and affects synaptic transmission as demonstrated during long-term potentiation of hippocampal CA1 perforant path synapses (Ahmed and Siegelbaum, 2009), during synapse maturation in the calyx of Held (Fedchyshyn and Wang, 2005) or in synapses where compensation by other channel types occurs upon genetic deletion of the naturally occurring one (Inchauspe et al., 2004, 2007). Thus, specific recruitment of $Ca_V2.1$ by Bassoon might play an important role in fine-tuning of synaptic transmission and occur during synaptic plasticity.

Different Roles for Bassoon in Regulating Synaptic Transmission

Bassoon was functionally linked to Ca^{2+} channel function in previous studies showing an aberrant alignment of presynaptic $Ca_V1.3$ at ribbon synapses of inner ear hair cells in *Bsn*$^{-/-}$ mice (Frank et al., 2010; Jing et al., 2013). $Ca_V1.3$ binds RBPs (Hibino et al., 2002) and thus could be regulated by Bassoon via RBPs at these synapses. Moreover, the release site reusage is decelerated in *Bsn*$^{-/-}$ mice (Frank et al., 2010; Hallermann et al., 2010), what might be at least partially caused by delayed release site reassembly due to impaired coupling to $Ca_V2.1$ in the absence of Bassoon. *Bassoon*-mutant mice suffer from rapidly generalizing epileptic seizures (Altrock et al., 2003; Ghiglieri et al., 2009). Mutations affecting function of $Ca_V2.1$ were also associated with epilepsy (Rajakulendran et al., 2012) suggesting that defect in $Ca_V2.1$-dependent synaptic transmission might contribute to the epileptic phenotype of *Bassoon* mutants. We observed a reduced spontaneous release from *Bsn*$^{-/-}$ neurons, which can partially be explained by impaired $Ca_V2.1$ recruitment (Ermolyuk et al., 2013). Moreover, this observation is in line with a reduction of the release-ready pool of synaptic vesicles in the absence of Bassoon (Altrock et al., 2003; Jing et al., 2013; Khimich et al., 2005). Although the underlying molecular mechanism remains to be clarified, it supports the view that the large presynaptic scaffold protein Bassoon is crucially involved in the molecular linkage of multiple steps of neurotransmitter release (Figure 8) mutually shaping presynaptic plasticity.

EXPERIMENTAL PROCEDURES

A detailed description of antibodies and other materials is provided in the Supplemental Information. Detailed methods for the generation of DNA constructs, library screening and mapping of interaction sites with the Y2H system, immunoblotting analyses and immunoprecipitation, surface plasmon resonance analyses, and electrophysiology are described in the Supplemental Experimental Procedures.

Cell Culture and Treatment

Corecruitment assays in COS7 cells using the mito-targeting system were performed essentially as described (Fejtova et al., 2009). Preparation of primary neurons from rat and mouse hippocampi and transfection using the Ca^{2+} phosphate method (rat) or Lipofectamine (mouse) are described in the Supplemental Information. *Bsn*$^{-/-}$ mice originating from Omnibank ES cell line OST486029 by Lexicon Pharmaceuticals were described previously (Hallermann et al., 2010). Immunostaining and synaptotagmin-antibody uptake assays in neurons were done as described earlier (Lazarevic et al., 2011). TAT-peptides (1 μM, TAT-WT: YGRKKRRQRRRPNGLVRKVKRTLPSP PPEEA and TAT-RBM: YGRKKRRQRRRPNGLVRKVKATLASPAPEEA) were added 2 hr before analysis directly to the culture medium. Details of treatment and pharmacology are reported in the Supplemental Information.

Image Acquisition and Analysis

Images were acquired with a confocal microscope (SP5; Leica). Figures 1B, 3A, 3E, 4A, 4E–4H, S1A, S1B, and S3A equipped with LCS software (Leica) or with an upright microscope (Axio Imager, Carl Zeiss). Figures 2C, 5B, 6A, and S5A–S5D equipped with a CCD camera (CoolSNAP EZ, Photometrics) and VisiView software (Visitron Systems GmbH).

In general, single images were acquired using camera or photomultiplier settings identically applied to all samples quantified in one experiment. Maximal projections of confocal stacks and threshold subtraction were done using NIH ImageJ software. Synapse definition and IF intensity measurement was performed semiautomatically using OpenView software (Tsuriel et al., 2006) as described in detail in the Supplemental Information. Details on the colocalization and synaptic density analysis, Pearson's correlation coefficient calculation, and measurement of synaptic and total IF for Ca_Vs are provided in the same section. Statistics were performed with Prism5 software (GraphPad Software,) using one-way ANOVA or Student's t test as indicated for each experiment. All results of quantitative analyses are given as means ± SEM in text and figures.

SUPPLEMENTAL INFORMATION

Supplemental Information includes Supplemental Experimental Procedures and six figures and can be found with this article online at http://dx.doi.org/10.1016/j.neuron.2014.02.012.

AUTHOR CONTRIBUTIONS

W.D.A. performed the initial Y2H screen. D.D., C.M., F.B., S.R., W.D.A., and A.F. designed, performed, and analyzed interaction studies. D.D., C.M., C.K., Y.K., R.S., C.H., M.S., C.M.-V., M.H. and A.F. designed, performed, and analyzed functional studies in neurons and brain slices. D.A.R. was involved in experimental design and analysis of field recordings in mutant mice and using TAT-peptides. D.D., C.M., E.D.G., and A.F. designed the study and wrote the paper. D.D. and C.M. contributed equally to this work. E.D.G. and A.F. share senior authorship. All authors discussed the results and commented on manuscript.

ACKNOWLEDGMENTS

We thank J. Juhle, B. Kracht, S. Opitz, and H. Wickborn for excellent technical support, C. Schöne, for help with mouse primary cultures, all members of the Magdeburg labs, R. Frischknecht and C.C. Garner for helpful discussions, and E. Neher for valuable comments on the manuscript. The study was supported by Deutsche Forschungsgemeinschaft (DFG) (SFB779/B9, GRK 1167 to E.D.G., AL1115 to W.D.A., FE1335/1 to A.F., and HE3604/2-1 to M.H.), the European Community (HEALTH-2007-22918, REPLACES), the State NRW (to C.H.), ERANET NEURON (AMRePACELL), and the European Regional Development Fonds and the Land Saxony-Anhalt (EFRE/LSA 2007-2013-ZVOH) to A.F. and E.D.G.

Accepted: January 28, 2014
Published: April 2, 2014

REFERENCES

Ahmed, M.S., and Siegelbaum, S.A. (2009). Recruitment of N-Type Ca(2+) channels during LTP enhances low release efficacy of hippocampal CA1 perforant path synapses. Neuron *63*, 372–385.

Altrock, W.D., tom Dieck, S., Sokolov, M., Meyer, A.C., Sigler, A., Brakebusch, C., Fässler, R., Richter, K., Boeckers, T.M., Potschka, H., et al. (2003). Functional inactivation of a fraction of excitatory synapses in mice deficient for the active zone protein bassoon. Neuron *37*, 787–800.

Anggono, V., Smillie, K.J., Graham, M.E., Valova, V.A., Cousin, M.A., and Robinson, P.J. (2006). Syndapin I is the phosphorylation-regulated dynamin I partner in synaptic vesicle endocytosis. Nat. Neurosci. *9*, 752–760.

Ariel, P., Hoppa, M.B., and Ryan, T.A. (2012). Intrinsic variability in Pv, RRP size, Ca(2+) channel repertoire, and presynaptic potentiation in individual synaptic boutons. Front. Synaptic Neurosci. *4*, 9.

Cao, Y.Q., and Tsien, R.W. (2010). Different relationship of N- and P/Q-type Ca2+ channels to channel-interacting slots in controlling neurotransmission at cultured hippocampal synapses. J. Neurosci. *30*, 4536–4546.

Cao, Y.Q., Piedras-Rentería, E.S., Smith, G.B., Chen, G., Harata, N.C., and Tsien, R.W. (2004). Presynaptic Ca2+ channels compete for channel type-preferring slots in altered neurotransmission arising from Ca2+ channelopathy. Neuron *43*, 387–400.

Catterall, W.A., and Few, A.P. (2008). Calcium channel regulation and presynaptic plasticity. Neuron *59*, 882–901.

Collins, M.O., Yu, L., Coba, M.P., Husi, H., Campuzano, I., Blackstock, W.P., Choudhary, J.S., and Grant, S.G. (2005). Proteomic analysis of in vivo phosphorylated synaptic proteins. J. Biol. Chem. *280*, 5972–5982.

Dresbach, T., Hempelmann, A., Spilker, C., tom Dieck, S., Altrock, W.D., Zuschratter, W., Garner, C.C., and Gundelfinger, E.D. (2003). Functional regions of the presynaptic cytomatrix protein bassoon: significance for synaptic targeting and cytomatrix anchoring. Mol. Cell. Neurosci. *23*, 279–291.

Ermolyuk, Y.S., Alder, F.G., Surges, R., Pavlov, I.Y., Timofeeva, Y., Kullmann, D.M., and Volynski, K.E. (2013). Differential triggering of spontaneous glutamate release by P/Q-, N- and R-type Ca2+ channels. Nat. Neurosci. *16*, 1754–1763.

Fedchyshyn, M.J., and Wang, L.Y. (2005). Developmental transformation of the release modality at the calyx of Held synapse. J. Neurosci. *25*, 4131–4140.

Fejtova, A., Davydova, D., Bischof, F., Lazarevic, V., Altrock, W.D., Romorini, S., Schöne, C., Zuschratter, W., Kreutz, M.R., Garner, C.C., et al. (2009). Dynein light chain regulates axonal trafficking and synaptic levels of Bassoon. J. Cell Biol. *185*, 341–355.

Frank, T., Rutherford, M.A., Strenzke, N., Neef, A., Pangršič, T., Khimich, D., Fejtova, A., Gundelfinger, E.D., Liberman, M.C., Harke, B., et al. (2010). Bassoon and the synaptic ribbon organize Ca^2+ channels and vesicles to add release sites and promote refilling. Neuron *68*, 724–738.

Ghiglieri, V., Picconi, B., Sgobio, C., Bagetta, V., Barone, I., Paillè, V., Di Filippo, M., Polli, F., Gardoni, F., Altrock, W., et al. (2009). Epilepsy-induced abnormal striatal plasticity in Bassoon mutant mice. Eur. J. Neurosci. *29*, 1979–1993.

Graf, E.R., Valakh, V., Wright, C.M., Wu, C., Liu, Z., Zhang, Y.Q., and DiAntonio, A. (2012). RIM promotes calcium channel accumulation at active zones of the Drosophila neuromuscular junction. J. Neurosci. *32*, 16586–16596.

Gundelfinger, E.D., and Fejtova, A. (2012). Molecular organization and plasticity of the cytomatrix at the active zone. Curr. Opin. Neurobiol. *22*, 423–430.

Hallermann, S., Fejtova, A., Schmidt, H., Weyhersmüller, A., Silver, R.A., Gundelfinger, E.D., and Eilers, J. (2010). Bassoon speeds vesicle reloading at a central excitatory synapse. Neuron *68*, 710–723.

Han, Y., Kaeser, P.S., Südhof, T.C., and Schneggenburger, R. (2011). RIM determines Ca^2+ channel density and vesicle docking at the presynaptic active zone. Neuron *69*, 304–316.

Hibino, H., Pironkova, R., Onwumere, O., Vologodskaia, M., Hudspeth, A.J., and Lesage, F. (2002). RIM binding proteins (RBPs) couple Rab3-interacting molecules (RIMs) to voltage-gated Ca(2+) channels. Neuron *34*, 411–423.

Higley, M.J., and Sabatini, B.L. (2008). Calcium signaling in dendrites and spines: practical and functional considerations. Neuron *59*, 902–913.

Holderith, N., Lorincz, A., Katona, G., Rózsa, B., Kulik, A., Watanabe, M., and Nusser, Z. (2012). Release probability of hippocampal glutamatergic terminals scales with the size of the active zone. Nat. Neurosci. *15*, 988–997.

Hoppa, M.B., Lana, B., Margas, W., Dolphin, A.C., and Ryan, T.A. (2012). $\alpha 2\delta$ expression sets presynaptic calcium channel abundance and release probability. Nature *486*, 122–125.

Inchauspe, C.G., Martini, F.J., Forsythe, I.D., and Uchitel, O.D. (2004). Functional compensation of P/Q by N-type channels blocks short-term plasticity at the calyx of held presynaptic terminal. J. Neurosci. *24*, 10379–10383.

Inchauspe, C.G., Forsythe, I.D., and Uchitel, O.D. (2007). Changes in synaptic transmission properties due to the expression of N-type calcium channels at the calyx of Held synapse of mice lacking P/Q-type calcium channels. J. Physiol. *584*, 835–851.

Iwasaki, S., Momiyama, A., Uchitel, O.D., and Takahashi, T. (2000). Developmental changes in calcium channel types mediating central synaptic transmission. J. Neurosci. *20*, 59–65.

Jing, Z., Rutherford, M.A., Takago, H., Frank, T., Fejtova, A., Khimich, D., Moser, T., and Strenzke, N. (2013). Disruption of the presynaptic cytomatrix protein bassoon degrades ribbon anchorage, multiquantal release, and sound encoding at the hair cell afferent synapse. J. Neurosci. *33*, 4456–4467.

Jun, K., Piedras-Rentería, E.S., Smith, S.M., Wheeler, D.B., Lee, S.B., Lee, T.G., Chin, H., Adams, M.E., Scheller, R.H., Tsien, R.W., and Shin, H.S. (1999). Ablation of P/Q-type Ca(2+) channel currents, altered synaptic transmission, and progressive ataxia in mice lacking the alpha(1A)-subunit. Proc. Natl. Acad. Sci. USA *96*, 15245–15250.

Kaeser, P.S., Kwon, H.B., Chiu, C.Q., Deng, L., Castillo, P.E., and Südhof, T.C. (2008). RIM1alpha and RIM1beta are synthesized from distinct promoters of the RIM1 gene to mediate differential but overlapping synaptic functions. J. Neurosci. *28*, 13435–13447.

Kaeser, P.S., Deng, L., Wang, Y., Dulubova, I., Liu, X., Rizo, J., and Südhof, T.C. (2011). RIM proteins tether Ca2+ channels to presynaptic active zones via a direct PDZ-domain interaction. Cell *144*, 282–295.

Khimich, D., Nouvian, R., Pujol, R., Tom Dieck, S., Egner, A., Gundelfinger, E.D., and Moser, T. (2005). Hair cell synaptic ribbons are essential for synchronous auditory signalling. Nature *434*, 889–894.

Kittel, R.J., Wichmann, C., Rasse, T.M., Fouquet, W., Schmidt, M., Schmid, A., Wagh, D.A., Pawlu, C., Kellner, R.R., Willig, K.I., et al. (2006). Bruchpilot promotes active zone assembly, Ca2+ channel clustering, and vesicle release. Science *312*, 1051–1054.

Kiyonaka, S., Wakamori, M., Miki, T., Uriu, Y., Nonaka, M., Bito, H., Beedle, A.M., Mori, E., Hara, Y., De Waard, M., et al. (2007). RIM1 confers sustained activity and neurotransmitter vesicle anchoring to presynaptic Ca2+ channels. Nat. Neurosci. *10*, 691–701.

Kraszewski, K., Mundigl, O., Daniell, L., Verderio, C., Matteoli, M., and De Camilli, P. (1995). Synaptic vesicle dynamics in living cultured hippocampal neurons visualized with CY3-conjugated antibodies directed against the lumenal domain of synaptotagmin. J. Neurosci. *15*, 4328–4342.

Lazarevic, V., Schöne, C., Heine, M., Gundelfinger, E.D., and Fejtova, A. (2011). Extensive remodeling of the presynaptic cytomatrix upon homeostatic adaptation to network activity silencing. J. Neurosci. *31*, 10189–10200.

Liu, K.S., Siebert, M., Mertel, S., Knoche, E., Wegener, S., Wichmann, C., Matkovic, T., Muhammad, K., Depner, H., Mettke, C., et al. (2011). RIM-

binding protein, a central part of the active zone, is essential for neurotransmitter release. Science *334*, 1565–1569.

Luebke, J.I., Dunlap, K., and Turner, T.J. (1993). Multiple calcium channel types control glutamatergic synaptic transmission in the hippocampus. Neuron *11*, 895–902.

Mayer, B.J. (2001). SH3 domains: complexity in moderation. J. Cell Sci. *114*, 1253–1263.

Missler, M., Zhang, W., Rohlmann, A., Kattenstroth, G., Hammer, R.E., Gottmann, K., and Südhof, T.C. (2003). Alpha-neurexins couple Ca2+ channels to synaptic vesicle exocytosis. Nature *423*, 939–948.

Mittelstaedt, T., and Schoch, S. (2007). Structure and evolution of RIM-BP genes: identification of a novel family member. Gene *403*, 70–79.

Müller, C.S., Haupt, A., Bildl, W., Schindler, J., Knaus, H.G., Meissner, M., Rammner, B., Striessnig, J., Flockerzi, V., Fakler, B., and Schulte, U. (2010). Quantitative proteomics of the Cav2 channel nano-environments in the mammalian brain. Proc. Natl. Acad. Sci. USA *107*, 14950–14957.

Munton, R.P., Tweedie-Cullen, R., Livingstone-Zatchej, M., Weinandy, F., Waidelich, M., Longo, D., Gehrig, P., Potthast, F., Rutishauser, D., Gerrits, B., et al. (2007). Qualitative and quantitative analyses of protein phosphorylation in naive and stimulated mouse synaptosomal preparations. Mol. Cell. Proteomics *6*, 283–293.

Murthy, V.N., Sejnowski, T.J., and Stevens, C.F. (1997). Heterogeneous release properties of visualized individual hippocampal synapses. Neuron *18*, 599–612.

Neher, E., and Sakaba, T. (2008). Multiple roles of calcium ions in the regulation of neurotransmitter release. Neuron *59*, 861–872.

Rajakulendran, S., Kaski, D., and Hanna, M.G. (2012). Neuronal P/Q-type calcium channel dysfunction in inherited disorders of the CNS. Nat. Rev. Neurol. *8*, 86–96.

Saheki, Y., and Bargmann, C.I. (2009). Presynaptic CaV2 calcium channel traffic requires CALF-1 and the alpha(2)delta subunit UNC-36. Nat. Neurosci. *12*, 1257–1265.

Scholz, K.P., and Miller, R.J. (1995). Developmental changes in presynaptic calcium channels coupled to glutamate release in cultured rat hippocampal neurons. J. Neurosci. *15*, 4612–4617.

Sgobio, C., Ghiglieri, V., Costa, C., Bagetta, V., Siliquini, S., Barone, I., Di Filippo, M., Gardoni, F., Gundelfinger, E.D., Di Luca, M., et al. (2010). Hippocampal synaptic plasticity, memory, and epilepsy: effects of long-term valproic acid treatment. Biol. Psychiatry *67*, 567–574.

Sheng, J., He, L., Zheng, H., Xue, L., Luo, F., Shin, W., Sun, T., Kuner, T., Yue, D.T., and Wu, L.G. (2012). Calcium-channel number critically influences synaptic strength and plasticity at the active zone. Nat. Neurosci. *15*, 998–1006.

Südhof, T.C. (2012). The presynaptic active zone. Neuron *75*, 11–25.

Takahashi, T., and Momiyama, A. (1993). Different types of calcium channels mediate central synaptic transmission. Nature *366*, 156–158.

Tsuriel, S., Geva, R., Zamorano, P., Dresbach, T., Boeckers, T., Gundelfinger, E.D., Garner, C.C., and Ziv, N.E. (2006). Local sharing as a predominant determinant of synaptic matrix molecular dynamics. PLoS Biol. *4*, e271.

Wang, Y., and Südhof, T.C. (2003). Genomic definition of RIM proteins: evolutionary amplification of a family of synaptic regulatory proteins(small star, filled). Genomics *81*, 126–137.

Wang, Y., Sugita, S., and Sudhof, T.C. (2000). The RIM/NIM family of neuronal C2 domain proteins. Interactions with Rab3 and a new class of Src homology 3 domain proteins. J. Biol. Chem. *275*, 20033–20044.

Wu, L.G., and Saggau, P. (1994). Pharmacological identification of two types of presynaptic voltage-dependent calcium channels at CA3-CA1 synapses of the hippocampus. J. Neurosci. *14*, 5613–5622.